Electrical Power and Energy Systems 43 (2012) 40–46

Contents lists available at SciVerse ScienceDirect

Electrical Power and Energy Systems

journal homepage: www.elsevier.com/locate/ijepes

Design and development of a model-based hardware simulator for photovoltaic array

A. Vijayakumari [a,*], A.T. Devarajan [a], N. Devarajan [b]

[a] Amrita Vishwa Vidyapeetham University, Coimbatore 112, India
[b] Government College of Technology, Coimbatore 13, India

ARTICLE INFO

Article history:
Received 21 September 2011
Received in revised form 14 January 2012
Accepted 23 April 2012
Available online 18 June 2012

Keywords:
Photovoltaic array
Hardware simulator
PV modeling
Insolation

ABSTRACT

This paper presents a model based hardware simulator to emulate a photovoltaic (PV) array/module for all operating conditions. For making the model accurate the values of manufacturer dependent parameters pertaining to a PV array are extracted from the published data sheet of the array by a curve fitting based extraction technique. The proposed simulator consists of a microcontroller controlled switched mode DC–DC converter. The mathematical model of the PV array is embedded in the controller with provisions for the user to enter the required ambient conditions. A feedback compensator is implemented to achieve fast response and good stability and to minimize the steady-state error. As a test case to design, develop and test for compliance the published data of 115 W solar panel Shell S115 has been used. The prototype is tested for steady-state and transient conditions. The experimental results of the simulator are presented. The results are compared with the cell characteristics available in literature and compliance is confirmed.

1. Introduction

The world wide, demand for electrical energy is growing fast, demanding the utilization of alternative and renewable energy sources. The increased use of distributed generation calls for the growth of associated power electronics; for example, to maximize the utilization of solar PV panels and to convert the dc power of the panel to suit the loads/grid requirements. For consistent performance of these PV power converters the experiments need to be repeated for every load/grid condition at every possible insolation, i.e. irradiance, G and temperature, T_C. This becomes difficult with a solar PV panel, as it is not practical to repeatedly set the steady-state and transient insolation at all values and as required. To perform intense testing of the PV power converter's functionality, its closed loop control, its performance when subjected to grid disturbances, a real-time hardware infrastructure is essential. Thus the simulator is primarily intended as a power source to the converter in experiments to verify the reliability and repeatability of operation of the converter in steady-state as well as in transient conditions of all possible insolation/grid conditions. Such a hardware simulator has to produce dc outputs effectively as will be given by a PV panel at any operating condition.

Wide varieties of hardware PV simulators have been reported in the literature. In [1,2] the output of a single photo sensor is magnified using linear amplifiers to emulate the PV array. No temperature variation has been considered. The series resistance, the ideality factor and reverse saturation current of cells in an array may be different from that of a single photo sensor that can cause errors in the model. The major drawback of this method is its lower efficiency due to linear amplification. This will be a serious concern for high power simulators.

The simulator in [3], uses a switching power converter with an analog control and matching only the open circuit and short circuit points of the simulator with those of the actual PV panel. Also changes in load conditions have only been considered and the changes in insolation have not been accounted. Using switching power converter, a digital control strategy is adapted in [4–5], in which a Look Up Table (LUT) is used to store the V–I relationship of a PV array for some discrete insolation conditions. The LUT is referred to for the control of the power converter so that the converter output is the same as the values in the table. No provision for accounting the change in insolation is reported in [4]. In [5] only three sets of insolation conditions are used which are manually selected. Variable insolation conditions are not realized. Different types of PV cell models are reported in [6–11], and model based emulators are reported in [12,13]. However [12], did not consider the changes in the ambient conditions while in [13] these were considered, but it is applicable for a particular site. The irradiance is given as an input to get the PV characteristics. The temperature

* Corresponding author. Address: Department of Electrical and Electronics Engineering, Amrita Vishwa Vidyapeetham University, Amrita Nagar, Coimbatore 641 112, India. Tel.: +91 4222656422, mobile: +91 9942999952.

E-mail addresses: a_vijayakumari@cb.amrita.edu, aviji71@yahoo.com (A. Vijayakumari).

0142-0615/$ - see front matter © 2012 Elsevier Ltd. All rights reserved.
http://dx.doi.org/10.1016/j.ijepes.2012.04.049

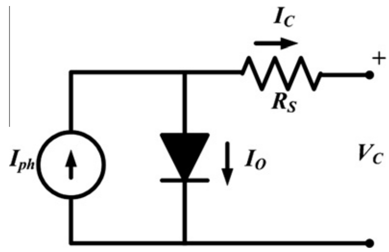

Fig. 1a. Equivalent circuit.

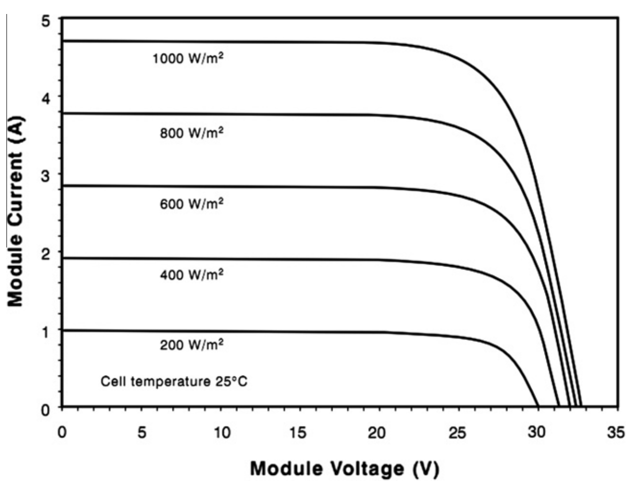

Fig. 1b. *V–I* characteristics of solar PV panel S115l.

is indirectly estimated from a site data. Thus it is dependent on the site data, and that constrains the universal use of the simulator.

This paper presents a model based hardware PV simulator, which emulates the *V–I* characteristics of a typical 115 W Shell solar PV module S115 for any temperature and irradiance conditions. The model parameters are extracted using only the published cell characteristics of the manufacturer. None of the values required for the cell equation has been assumed as has been done often in the literature [14–17], thus the model replicates the commercial PV panel very closely. The emulator uses the model for obtaining the *V–I* relationships, thus no look up tables are used requiring large memories. This enables to obtain the characteristics at any insolation conditions, compared to [3–5] where, emulation at certain discrete insolation is only reported. First the mathematical modeling of a commercial PV array is explained followed by the design specification of the converter used in the simulator. Finally the development of the hardware setup and the experimental results are presented. The simulator can be used for testing of power converters for PV applications where it can replace the actual panel at any desired insolation level as well as for testing of various Maximum Power Point Tracking (MPPT) algorithms.

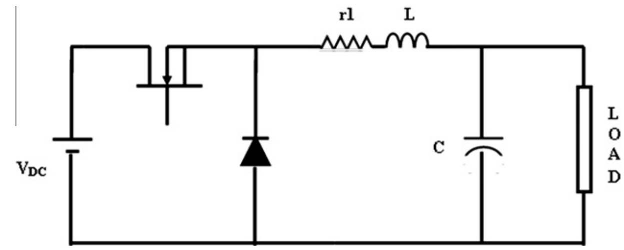

Fig. 3. Power circuit of PV simulator.

2. Mathematical model of PV panel

The equivalent circuit of a solar cell is given in Fig. 1a. The *V–I* characteristics [18] of a solar module (S115) are given in Fig. 1b.

The output voltage of a single solar cell [14] in volts is expressed as

$$V_C = \frac{AkT_C}{e} \ln\left(\frac{I_{ph} + I_O - I_C}{I_O}\right) - R_S I_C \quad (1)$$

where A is diode ideality factor, I_{ph} is photocurrent (A), I_O is reverse saturation current (A), e is electron charge (Q), R_S is series resistance of the cell (Ω), k is Boltzmann's constant, T_C is cell operating temperature in Kelvin, V_C is cell output voltage (V), I_C is cell output current (A).

The values of the manufacture-dependent parameters viz, I_{ph}, I_O, A and $R_{S,}$ pertaining to a particular PV panel are extracted from the *V–I* characteristics published in the data sheet of that particular PV panel. A curve fitting based extraction technique is adapted in this paper.

The first unknown parameter I_{ph} in (1) is seen to be equal to I_C under short circuit of panel as drop in R_S is too small to make the

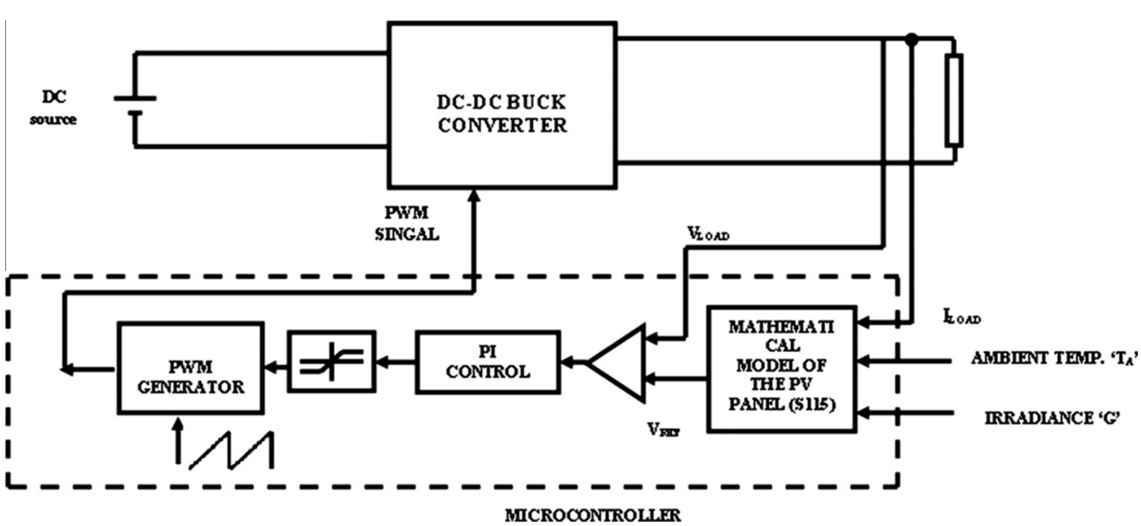

Fig. 2. The proposed hardware PV simulator.

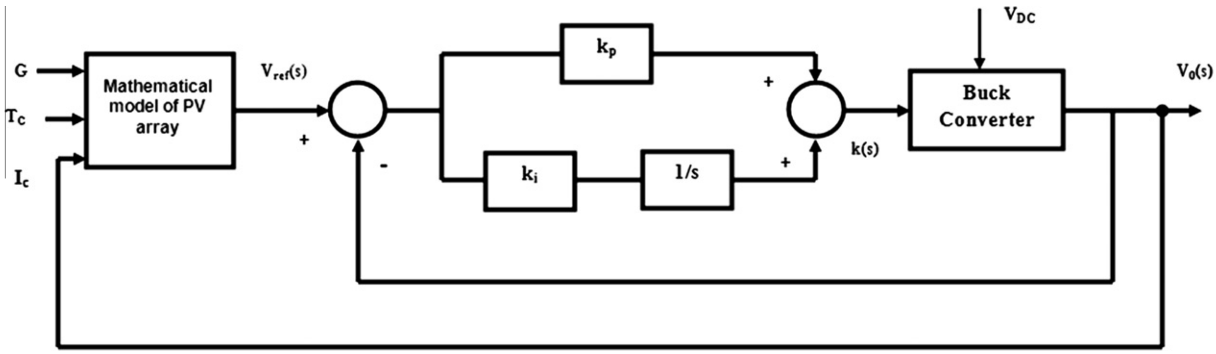

Fig. 4. Control of the converter.

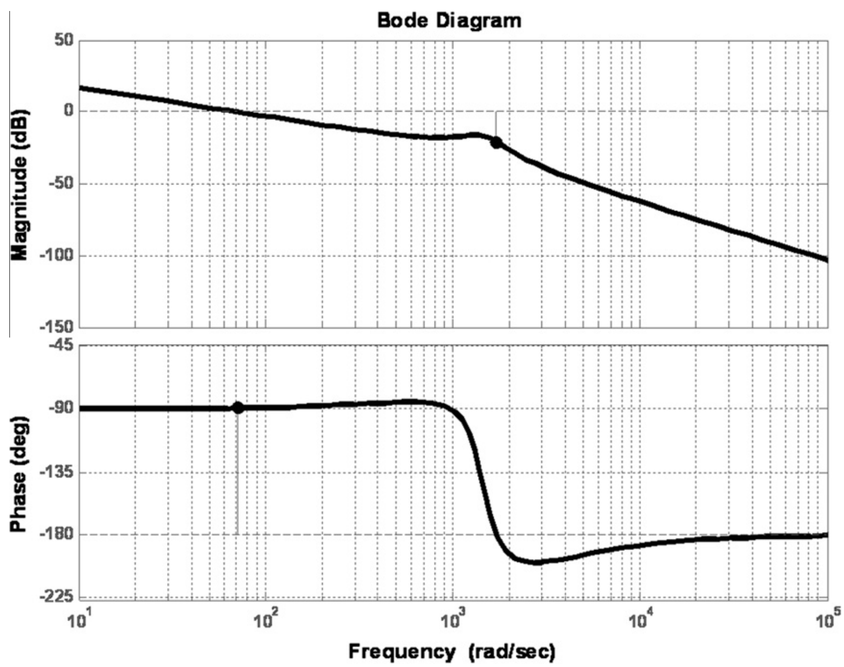

Fig. 5. Bode plot of the PI controlled buck converter.

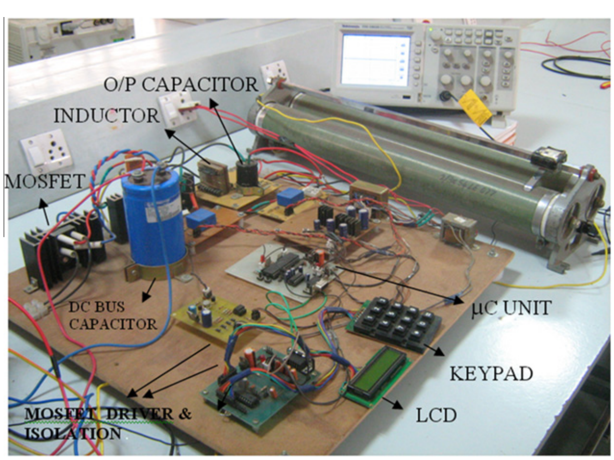

Fig. 6. The hardware simulator.

diode conduct any significant value. From the module's short circuit current I_{sc}, and the number of parallel branches N_P in the module, I_{ph} for a cell is found as I_{sc}/N_P. The remaining three process dependent parameters for the model are estimated through careful curve fitting of the data sheet characteristics by selecting three points on the published characteristic curve at Standard Test Condition (STC) for the module of interest. As the solar arrays are to be operated at MPP, the model as well as the emulator has to be more accurate near MPP. So the first point is selected at MPP. The second and the third points are selected at the left of MPP and at the right of MPP. The three points for Shell solar 'S115' chosen for verification of the model are $P_1(V_1 = 26.80\text{ V}, I_1 = 4.29\text{ A})$, $P_2(V_2 = 25.74\text{ V}, I_2 = 4.43\text{ A})$ and $P_3(V_3 = 27.93\text{ V}, I_3 = 4.06\text{ A})$ on the published V–I characteristics. Substitution of the co-ordinates of P_1, P_2 and P_3 suitably scaled down to a single cell value, in (1) gives the values for the three unknown parameters as $I_O = 9.25 \times 10^{-6}$ A, $A = 1.8$ and $R_S = 0.000192\ \Omega$.

The value of V_C can now be evaluated from (1) for any current I_C at STC. Then correction in voltage ΔV_C due to change in irradiance and the consequential change in cell current ΔI_C and temperature are introduced to get cell voltage V_C at any irradiance to complete the model.

At a given irradiance G, whenever the ambient temperature (T_A) varies, it causes the cell temperature (T_C) to vary. Also the change

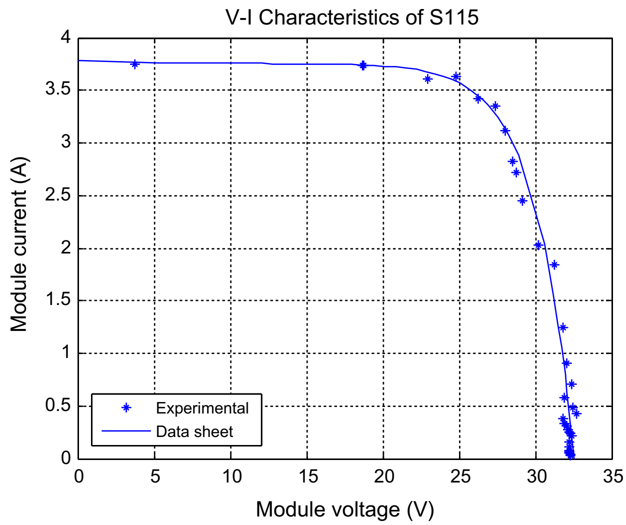

(a) $T_C = 25^0C$, $G = 800W/m^2$

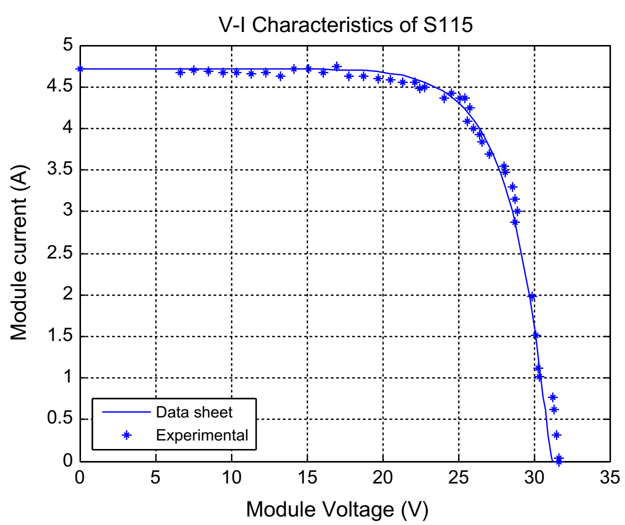

(b) $T_C = 40^0C$, $G = 800W/m^2$

Fig. 7. (a and b) *V–I* characteristics at different insolations.

in G causes change in cell current (ΔI_C) and cell temperature (ΔT_C) [19]. Finally these changes cause a change in cell voltage (ΔV_C) which is evaluated in volts as:

$$\Delta V_C = -\alpha_{VOC}\Delta T_C - R_S\Delta I_C \tag{2}$$

where α_{VOC} is the temperature coefficient of voltage, available in the data sheet. ΔI_C in Amperes and ΔT_C in Kelvin caused at any G are evaluated as:

$$\Delta I_C = \beta_{ISC}\left(\frac{G}{G_{stc}}\right)\Delta T_C + \left(\frac{G}{G_{stc}} - 1\right)I_{SC,stc} \tag{3}$$

$$\Delta T_C = T_C - T_{stc} \tag{4}$$

where β_{ISC} is the temperature coefficient of current from data sheet, T_C is the cell temperature at any irradiance and T_{stc} is the cell temperature at STC.

The cells operate at a higher temperature than the ambient [20]. The cell temperature T_C in Kelvin at any irradiance G is found as:

$$T_C = T_A + \left(\frac{T_{NOCT} - 20}{G_{NOCT}}\right)G \tag{5}$$

where T_A is the ambient temperature, T_{NOCT} is the normal operating cell temperature and G_{NOCT} is irradiance at NOCT. Both are available from the data sheet. Then the cell output voltage in volts and current in amperes for any required G and T_C are obtained as:

$$V_C = V_{C@STC} + \Delta V_C \tag{6}$$

$$I_C = I_{C@STC} + \Delta I_C \tag{7}$$

The cell model includes (1)–(7) and gives the cell voltage for a given cell current at any T_A and G. Thus the cell model calculates the cell voltage, for a given cell current. The panel voltage and current are calculated using the number of series cells in a string and number of parallel strings in a module.

3. Description of the simulator system

The block diagram of the hardware PV simulator is shown in Fig. 2. The circuit consists of a DC–DC buck converter fed from a dc source and controlled by PIC 16F877 microcontroller. The mathematical model of the PV array with parameters extracted from the actual panel is implemented in the microcontroller program.

The user defined inputs for the system are the ambient temperature T_A and Irradiance G. The required insolation values are entered into the model through a keypad and the same are displayed in LCD. The third input to the simulator is the load current, which serves as the PV module current for the mathematical model. With these three inputs the micro controller estimates the panel output voltage using the model. This is the reference voltage and the actual output voltage from the converter is the feedback signal for the closed loop system. The voltage error is used to control the converter output voltage such that the simulator output will be same as the voltage estimated by the mathematical model for the given current and the entered insolation.

4. Hardware design

The buck converter shown in Fig. 3 is used as the power stage for the proposed simulator. The output voltage and current of the converter should be equal to the array voltage and current, at any operating condition.

The hardware simulator is designed to represent the solar panel S115 for demonstration. The salient details [18] of the S115 are V_{OC} = 32.8 V, I_{sc} = 4.7A, V_{MPP} = 26.8 V, P_{MPP} = 115 W. For the buck converter a 35 V, 5 A power supply is used as an input. The switching frequency (f_{sc}) of the DC–DC converter is decided based on the switching frequency (f_{si}) of the interfacing inverter sourced from the PV simulator. Corresponding to a typical value of 5 kHz, a reasonable switching frequency value for the inverter, a switching frequency of 20 kHz is selected for the DC–DC converter. As these frequencies are far away, the interaction between the emulator and the interfacing converter will be minimum [21].

The buck converter is designed for continuous current operation with a steady-state peak to peak inductor current (Δi) and voltage ripple (Δv) of 5% and 0.5% respectively. With the chosen f_{sc} of 20 kHz, the values of the filter elements are designed based on equations

$$V_0 = V_{DC}k \tag{8}$$

$$\Delta i = \frac{kV_{DC}(1-k)}{f_{sc}L} \tag{9}$$

$$\Delta v = \frac{V_{DC}k(1-k)}{8LCf_{sc}^2} \tag{10}$$

where k is the duty ratio, V_{DC} is dc input voltage, L is the filter inductor and C is the filter capacitor.

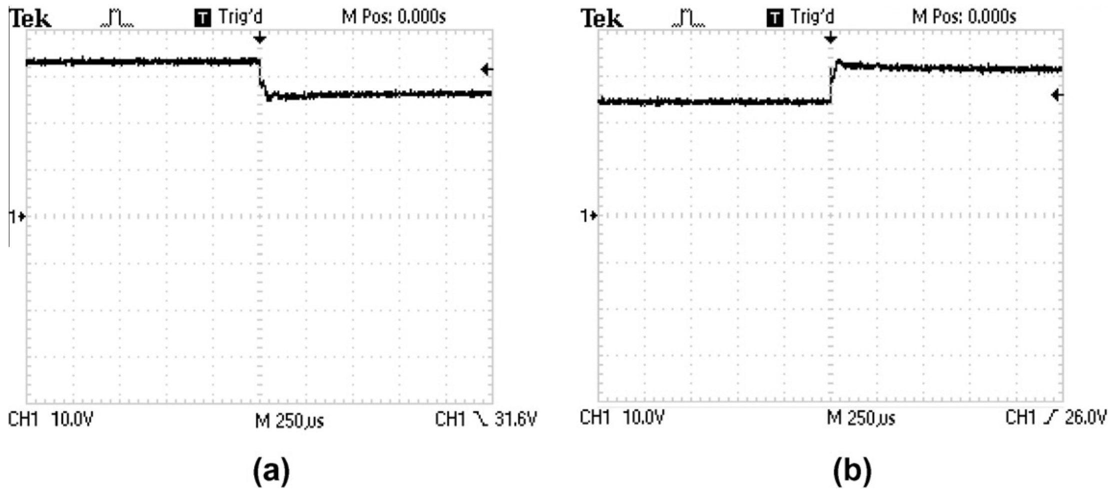

Fig. 8. Output voltage for step load change (a) from R_{OC} to R_{MPP} and (b) from R_{MPP} to R_{OC} under $G = 1000\ \mathrm{W/m^2}$, $T_C = 25\ ^\circ\mathrm{C}$.

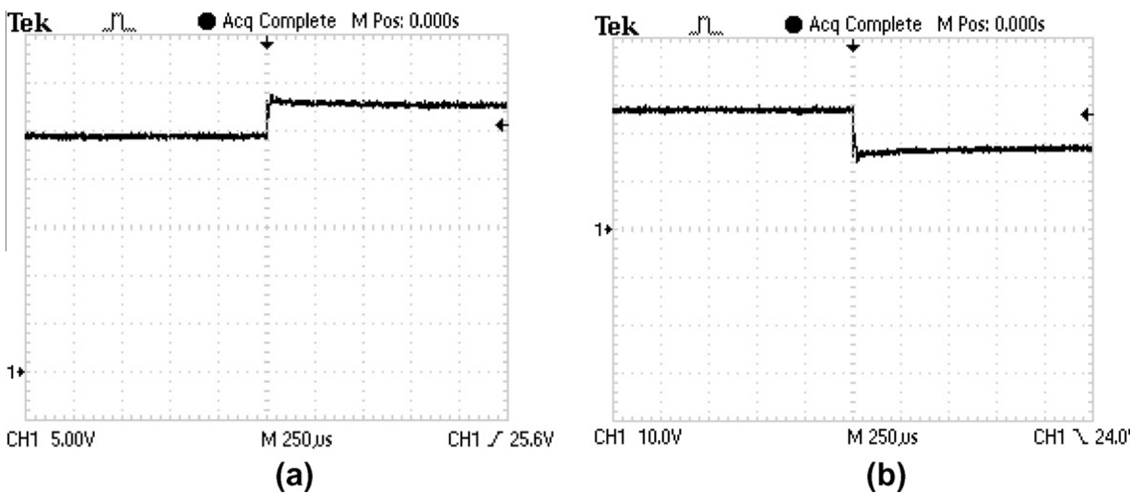

Fig. 9. Output voltage for step change in G. (a) From $800\ \mathrm{W/m^2}$ to $1000\ \mathrm{W/m^2}$ at $T_C = 40\ ^\circ\mathrm{C}$ and (b) from $800\ \mathrm{W/m^2}$ to $400\ \mathrm{W/m^2}$ at $T_C = 60\ ^\circ\mathrm{C}$.

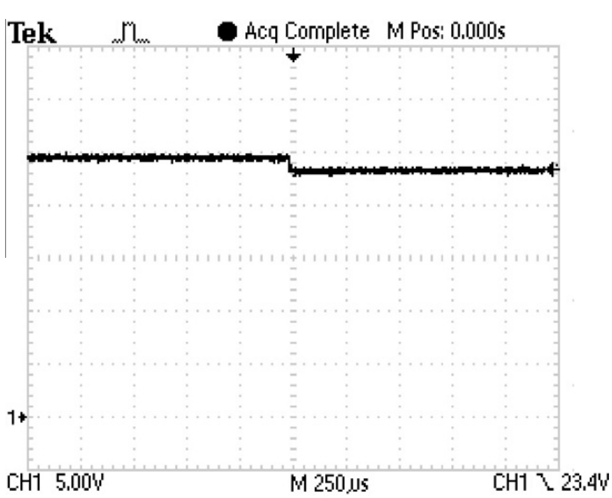

Fig. 10. Output voltage for step change of T_C from $20\ ^\circ\mathrm{C}$ to $60\ ^\circ\mathrm{C}$ with $G = 1000\ \mathrm{W/m^2}$.

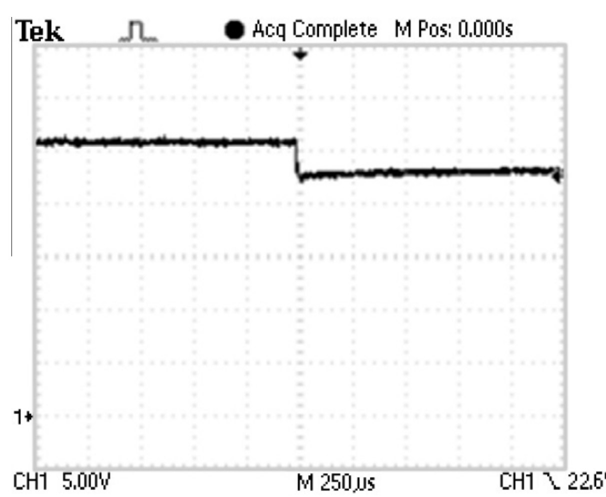

Fig. 11. Output voltage for step change of insolation from STC to NOCT.

The minimum values of L and C are found as 1.45 mH and 1.97 μF respectively. The inductor is fabricated and its internal resistance r_L is measured as 0.14 Ω. Instead of the calculated minimum C of 1.97 μF, 330 μF is used so as to improve the transient response under step load conditions.

Fig. 4 shows the closed loop control of the buck converter, which includes the PI controller acting as the compensator for the converter.

The compensator is so designed that (i) the gain at low frequencies is high to minimize the steady-state error in the output of the converter and (ii) the crossover frequency as high as possible for fast response and the phase margin is large enough to allow good stability. A value of 90° is chosen for phase margin as stability is more important in a grid connected system.

The converter transfer function $G_P(s)$ and the compensator transfer functions $G_C(s)$ are given as

$$G_P(s) = \frac{V_{Dc}}{LC\left[s^2 + s\left(\frac{1}{CR} + \frac{r_L}{L}\right) + \frac{1}{LC}\right]} \tag{11}$$

$$G_C(s) = \frac{k_p s + k_i}{s} \tag{12}$$

The values of k_p and k_i are designed as 0.001 and 2 respectively, so as to achieve the above mentioned design features.

The bode plot of the open loop transfer functions $G_P(s)$ $G_C(s)$ of the converter system given in Fig. 5 shows the phase margin as 90.9° at a cross over frequency of 70.2 rad/s

The experimental set up for the simulator is built to represent Shell solar module S115. The experimental set up consists of a DC–DC buck converter, which employs two power MOSFETs one as a switch and the other as the freewheeling diode, and a low pass filter with values as follows: L = 1.45 mH, C = 330 μF, r_L = 0.14 Ω.

The mathematical equations which depict the PV panel are coded in PIC16F877 microcontroller, operated with a clock frequency of 20 MHz. Fig. 6 shows the experimental set up of the hardware simulator. The LCD and keypad are interfaced with the microcontroller, so that the values are entered through keypad to one of the input ports. The third input, i.e. the load current is sensed using a Hall effect sensor and given to the built in ADC of the microcontroller. The calculations to determine the reference voltage takes far less than 50 μs by the controller, thus the input quantities, i.e. current and voltage are sampled at 50 μs interval. The comparator and the discrete PI controller are also programmed in the microcontroller.

5. Performance of the simulator

The static V–I characteristics of the simulator has been obtained to validate its performance under steady-state and transient conditions. The transient response of the hardware simulator has been obtained by (i) switching between two different load levels, (ii) introducing a sudden change in the ambient temperature and (iii) introducing a sudden change in the irradiance.

For obtaining steady-state characteristics, load test is conducted on the Simulator and the voltage and current values has been obtained experimentally and plotted for different sets of ambient conditions. In Fig. 7a and b the steady-state V–I characteristics of the hardware PV simulator are presented and compared with the data sheet. The experimental data and the data sheet values are matched using a 9th degree polynomial curve fit, and the deviation between them is found to be 0.5–1.5% for different insolations.

The dynamic response of the Simulator is obtained for change in the load resistance as well as change in the irradiance. The response of the PV simulator for a load change is experimentally obtained by switching a load resistance using a MOSFET switch. The load is switched from maximum power point load R_{MPP} = 6.3 Ω to open circuit R_{OC} at G = 1000 W/m^2, T_C = 25 °C. It is observed that the output voltage switches between its maximum power point voltage, V_{MPP} to open circuit voltage, V_{OC}. This is given in Fig. 8a and b.

Fig. 9a and b gives the dynamic change in output voltage when there is an increase and decrease in irradiance respectively with constant temperature. Fig. 10 gives the dynamic change in output voltage for change in cell temperature with constant irradiance. In each case the load resistance was kept as R_{MPP} corresponding to the initial insolation condition.

Fig. 11 gives the dynamic change in output voltage when the insolation changes from STC, i.e. G = 1000 W/m^2 and T_C = 25 °C, to NOCT, i.e. G = 800 W/m^2 and T_C = 44 °C. Finally in Fig. 12 the output voltage of the simulator for a step change in G from 200 W/m^2 to 1000 W/m^2 and vice versa are presented. The response time of the emulator is found to be in the range of 50–150 μs for various step insolation changes.

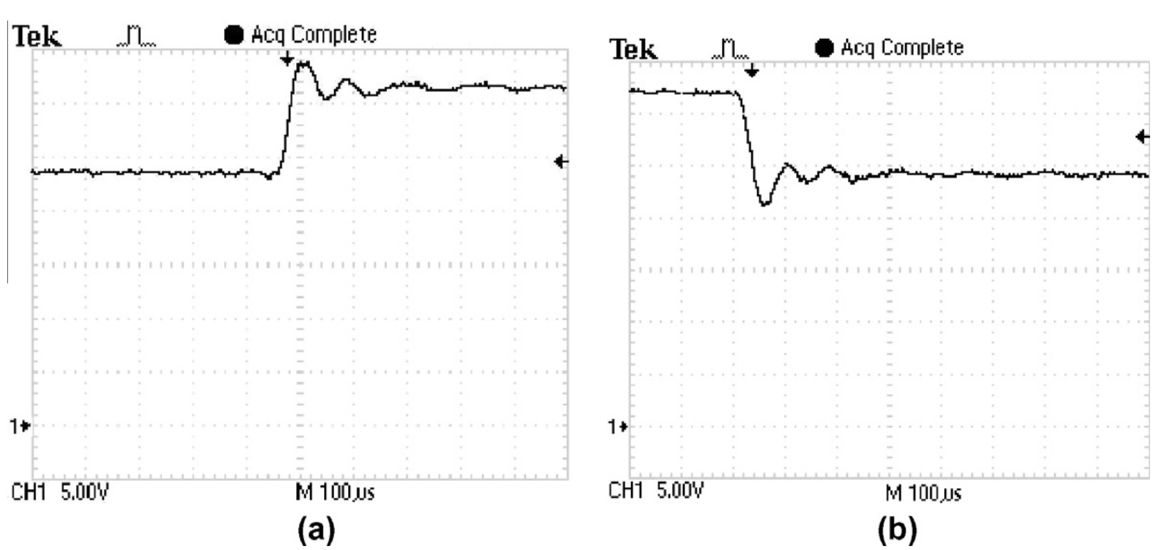

Fig. 12. Output voltage for step change in G. (a) From 200 W/m^2 to 1000 W/m^2 at T_C = 24 °C and (b) from 1000 W/m^2 to 200 W/m^2 at T_C = 25 °C.

6. Conclusion

A model based hardware PV simulator has been built and tested in the laboratory. The simulator uses a mathematical model that can be tailored to match any commercially available panel. The model based simulator gives *V–I* characteristics as that of any PV panel at any specified ambient conditions. The ambient conditions, as required by the operator can be input into the simulator system. As a test case the published data of 115 W solar panel Shell S115 has been used to build the simulator. The prototype has been tested in the laboratory for steady-state and transient conditions of insolation and load. For step change of insolation the output voltage is seen to change in 50–150 μs. This is as expected, as there is no appreciable time constant involved in a PV cell. The results are compared with the cell characteristics available in the literature and compliance is confirmed. The simulator is very useful as an input power source for testing of converters designed to interface PV panels to a load, especially when load is a utility grid.

Acknowledgments

The authors wish to acknowledge the contributions of Ms. Mintu V. Mani and Ms. S. Parvathy, Amrita School of Engineering, in the development of hardware circuits.

References

[1] Nagayoshi' Hiroshi, Orio Shinji, Kono Yuji, Nakajima Hirotaka. Novel PV array/module *I–V* curve simulator circuit. 29th IEEE PVSC 2002. http://dx.doi.org/10.1109/PVSC.2002.1190904.
[2] Nagayoshi Hiroshi. Characterization of the module/array simulator using *I–V* magnifier circuit of a PN photo-sensor, 3rd world conference on photovoltaic. Energy Convers 2003;2:2023–6.
[3] Ollila Jaakko. A medium power PV array simulator with a robust control strategy. 4th IEEE CCA 1995:40–5.
[4] Koutroulis Eftichios, Kalaitzakis Kostas, Tzitzilonis Vasileios. Development of an FPGA-based system for real-time simulation of photovoltaic modules. IEEE RSP 2006:200–7.
[5] Li Yuan, Lee Taewon, Peng FZ, Liu Dichen. A hybrid control strategy for photovoltaic simulator. IEEE APEC 2009:899–903.
[6] Tsai HL, Liang Huan. Insolation oriented model of photovoltaic module using matlab/simulink. Sol Energy 2010;84:1318–26.
[7] Pon Venkatesh R, Edward Rajan S. Investigation of cloud less solar radiation with PV module employing matlab/simulink. Sol Energy 2011;85:1727–34.
[8] Veerachary Mummadi. PSIM circuit-oriented simulator model for the nonlinear photovoltaic sources. IEEE Trans Aerospace Electronic Syst April 2006;42(2):735–40.
[9] Ishaque Kashif, Salam Zainal. An improved modeling method to determine the model parameters of photovoltaic (PV) modules using differential evolution (DE). Sol Energy 2011;85:2349–59.
[10] Carrero C, Rodriguex J, et al. Simple estimation of PV modules loss resistances for low error modeling. Renew Energy 2010;35:1103–8.
[11] Chang Ying-Pin. Optimal the tilt angles for photovoltaic modules in Taiwan. IJEPES Nov 2010;32(9):956–64.
[12] Martin-Segura G, Lopez-Mestre J, Teixido-Casas M, Sudria-Andreu A. Development of a photovoltaic array emulator system based on a full-bridge structure. EPQU 2007:1–6.
[13] Di Piazza MC, Pucci M, Ragusa A, Vitale G. Analytical versus neural real-time simulation of a photovoltaic generator based on a DC–DC converter. IEEE Trans Ind Appl 2010;46(6):2501–10.
[14] Atlas IH, Sharaf AM. A photovoltaic array simulation model for MATLAB-simulink GUI environment. PESC 2007:341–5.
[15] Ramasamy M, Thangavel S. Photovoltaic base dynamic voltage restorer with power saver capability using PI controller. IJEPES Mar 2012;36(1):51–9.
[16] Mazouz N, Midoun A. Control of dc–dc converter by fuzzy controller for a solar pumping system. IJEPES Dec 2011;33(10):1623–30.
[17] Mohamed Faisal A, Koivo Heikkl N. System modeling and online management of microgrid using mesh adaptive direct search. IJEPES June 2010;32(5):398–407.
[18] Shell Solar S115 Photovoltaic Solar Module, SAP Ref: 400353. <www.shellsolar.com>.
[19] Nikraz Magid, Dehbonei Hooman, Nayar Chem. A DSP-controlled photovoltaic system with maximum power point tracking. AUPEC 2003. Archive: itee.uq.edu.au, Paper No. 129; 2003.
[20] Roger A. Messenger and jerry venture, Photovoltaic systems engineering. 2nd ed. CRC Press; 2003.
[21] Mohan Ned, Underland Tore M, Robbins William P. Power electronics converters, applications and design. John Wiley & Sons; 2001.